



# Commercial plant protein isolates: The effect of insoluble particles on gelation properties

Senna W.P.M. Janssen<sup>a,\*</sup>, Laurice Pouvreau<sup>b</sup>, Renko J. de Vries<sup>a</sup>

<sup>a</sup> Physical Chemistry and Soft Matter, Wageningen University & Research, Wageningen, 6708WE, the Netherlands

<sup>b</sup> Wageningen Food & Biobased Research, Wageningen University & Research, Wageningen, 6709WG, the Netherlands

## ARTICLE INFO

### Keywords:

Commercial plant protein isolates  
Insoluble fraction  
Gelation  
Homogenization

## ABSTRACT

Commercial plant protein isolates generally contain a substantial fraction of large insoluble protein particles. We study how these affect the gelation properties of heat-induced protein gels (15% w/w protein, pH 7) and used homogenization as a mean to reduce the particle size of the insoluble fraction before gelation. Three different commercial plant proteins were studied as models for isolates differing in dispersibility and size of insoluble protein particles: Fava bean (FBPI), Pea (PPI) and Mung bean (MBPI). As expected, homogenization (50 MPa, 2 cycles) reduced the particle size and improved the dry matter dispersibility of protein dispersions. We found that the (shear) storage modulus  $G'$  and critical shear strain for fracture of gels obtained after heating were not consistently impacted by homogenization. In contrast, fracture properties in uniaxial compression were sensitive to homogenization, with homogenization leading to gels that are more resistant to fracture. Gels obtained from the isolate with the smallest fraction of insoluble particles and still contained native proteins, FBPI, were the most fracture resistant. Fluorescence microscopy indicated that the insoluble fraction remained well-dispersed in the matrix after heat-induced gelation and that homogenization led to a more homogeneous appearance of the protein networks, with smaller particles being homogeneously dispersed in the continuous background. We conclude that mechanically breaking down insoluble particles in commercial plant protein isolates contributes strongly to their functionality by reducing the number of large insoluble particles that act as effective nucleation points for hydrogel fracture.

## 1. Introduction

Plant protein functionality is rapidly gaining interest as a topic in current food science. This is the result of the growing role of plant proteins in providing healthy food for the growing world population in a sustainable way (Aiking & de Boer, 2020; Day, Cakebread, & Loveday, 2022; Sun-Waterhouse, Zhao, & Waterhouse, 2014). A key functionality of proteins in food is to provide structure and texture by network formation, for example by heat-induced gelation. Although the propensity for heat-induced gelation varies strongly among various plant protein sources, most of the currently used commercial plant protein isolates have rather poor gelling properties (Johansson et al., 2021; Shand, Ya, Pietrasik, & Wanasundara, 2007).

The legume soy is often used as a benchmark in plant protein gelation due to the relatively good gelling and structuring behaviour of soy proteins, in contrast to other legume and oilseed proteins (Berghout, Boom, & van der Goot, 2015). However, there is a strong interest in

diversifying plant protein sources, for example in view of concerns around allergenicity, sustainability and GMO-status of soy proteins (Ong et al., 2022). Other protein sources that exhibit excellent gelling properties include leaf proteins, such as RuBisCO (Martin, Nieuwland, & De Jong, 2014). These indeed require a rather low critical concentration for gel formation, but unfortunately, RuBisCO and similar proteins are not yet commercially available at large scale and competitive prices.

Therefore, a key question remains how to get the maximum functionality out of the less than ideal plant protein isolates currently available and used in food industry. It is widely agreed that to a large part, loss of the innate functionality of commonly used commercial legume proteins such as pea, occurs during the processing steps required for isolate production. These include alkaline protein solubilization, isoelectric precipitation, heating and spray-drying. Conditions in these steps can be harsh (e.g. extreme pH, pasteurization or sterilization to ensure microbiological safety) leading to protein denaturation, aggregation, insolubility and hence to lower functionality (J. Yang,

\* Corresponding author.

E-mail addresses: [senna.janssen@wur.nl](mailto:senna.janssen@wur.nl) (S.W.P.M. Janssen), [laurice.pouvreau@wur.nl](mailto:laurice.pouvreau@wur.nl) (L. Pouvreau), [renko.devries@wur.nl](mailto:renko.devries@wur.nl) (R.J. de Vries).

<https://doi.org/10.1016/j.foodhyd.2024.110049>

Received 3 November 2023; Received in revised form 27 March 2024; Accepted 28 March 2024

Available online 29 March 2024

0268-005X/© 2024 The Authors. Published by Elsevier Ltd. This is an open access article under the CC BY license (<http://creativecommons.org/licenses/by/4.0/>).

Mocking-Bode, et al., 2022).

Many scientific studies on the functional properties of plant proteins are not performed with commercial protein isolates, but with fractions obtained from milder (lab scale) isolation procedures. This generally leads to preparations with an overall higher functionality and a lower fraction of insoluble particles. Indeed, solubility is a prerequisite for gelation capacity (Nicolai & Chassenieux, 2019; Shand et al., 2007). Some studies that do use (commercial) plant protein isolates first remove the insoluble fraction, for example by using centrifugation (Jo, Huang, & Chen, 2020; McCann, Guyon, Fischer, & Day, 2018). It has been suggested that one approach to improve gelling properties is to separate soluble and insoluble protein fractions and remix them at different ratios to tailor functionality, since these fractions have significantly different physicochemical properties (Moll, Salminen, Seitz, Schmitt, & Weiss, 2022). However, this would not be economical at industrial scale.

While many protein treatment strategies exist (chemical, enzymatic, physical) that one could consider to maximize the functionality of commercial plant protein isolates, very few of these are yet feasible and economical at industrial scale. (Sun-Waterhouse et al., 2014). A notable exception is high pressure homogenization, which is known to enhance the functional properties of proteins and other biomacromolecules. Homogenization and shear treatment are common processing steps at industrial level, but the impact of these treatments on the food functionality of the proteins, for example the resulting mechanics of heat-set gels, has not been characterized very well and is poorly understood.

During homogenization, fluid is pressurized through a narrow valve, disrupting particles by hydrodynamic cavitation, turbulence and shear forces (Ong et al., 2022; Sahil, Madhumita, Prabhakar, & Kumar, 2022; Sun-Waterhouse et al., 2014). In scientific literature often relatively high pressures are used to explore the effect of homogenization on protein functionality. However, moderate pressures (20–50 MPa) are more conventionally used in food industry processes and should therefore also be considered (Luo, Wang, et al., 2022). Additionally, while homogenization at moderate pressures may decrease particle size and increase the solubility of various plant proteins, extensive homogenization at high pressures can also have the opposite effects of promoting aggregation and a decreasing solubility (Levy, Okun, Davidovich-Pinhas, & Shpigelman, 2021; Luo, Cheng, Zhang, & Yang, 2022; Melchior, Moreton, Calligaris, Manzocco, & Nicoli, 2022; Ong et al., 2022; Sahil et al., 2022; Saricaoglu, 2020; Shkolnikov Lozober, Okun, & Shpigelman, 2021; Yang, Liu, Zeng, & Chen, 2018). Finally, to be relevant for the food industry, the effect of homogenization should be studied for dispersions of relatively high protein concentration to connect to processes for producing products such as plant-based yoghurts and cheeses.

In earlier studies on the impact of homogenization on gelation properties, the emphasis was on the linear rheological properties of the heat-induced gels. In these studies, it was found that homogenization may increase the shear modulus  $G'$  of heat-set gels (Kang et al., 2022; Luo, Cheng, et al., 2022; Ong et al., 2022; Saricaoglu, 2020; Zhao, Liu, & Xue, 2023). Specifically, it was reported (Ong et al., 2022) that 15% w/w commercial pea protein, which was dispersed by only stirring, could not form a self-standing heat-induced gel. While after homogenization of the protein, freeze-drying, re-dispersion and subsequent heating, self-standing gels were formed. In another study (Luo, Cheng, et al., 2022), it was observed that homogenization of lab-extracted quinoa protein isolate affected both the small and large deformation rheology, leading to an increase in complex modulus and increase of the strain at break for 5% w/w heat-set gels. Regarding the dependence on the pressure of homogenization, it has been shown (Saricaoglu, 2020) that homogenization can lead to more pronounced heat-induced gelation of lentil proteins, but only up to a certain pressure. Only a few other authors used penetration or compression tests to characterize the mechanics of heat-induced plant protein gels and found that homogenization treatments increased gel strength for respectively, lupin and 11S soy

globulin (Bader, Bez, & Eisner, 2011; Kang et al., 2022).

Most of the above studies did not use commercial plant protein isolates, and most did not comprehensively characterize the effects of homogenization on both linear and non-linear rheology of heat-induced plant protein gels. Neither did these studies relate mechanical changes to changes to the microstructure, for a range of protein sources. Therefore, we here aim to comprehensively study the effect of the insoluble fraction (by comparing samples with and without homogenization) on both the linear and non-linear rheology of heat-induced plant protein gels, in relation to their microstructure as characterized using confocal scanning laser microscopy (CSLM). We do so for three heat-induced commercial plant protein isolate gels: Fava bean, Pea and Mung bean.

These were chosen as models for commercial isolates with varying degrees of dispersibility: the particular Mung bean isolate that we used was poorly dispersible and had a substantial fraction of insoluble particles. In this study, to be able to properly disperse this powder, we performed an additional bead milling step before dispersion. In contrast, the Fava bean isolate that we used was very dispersible and had only a small amount of insoluble particles. Finally, the pea protein isolate that we used had a dispersibility in between the dispersibility of FBPI and MBPI. Our comprehensive study points to a very clear negative role for large insoluble particles in the crucially important fracture properties of heat-induced plant protein gels.

## 2. Materials & methods

### 2.1. Materials

Commercial plant protein isolate of Fava bean (FBPI) was obtained from Cosun Protein (Fava HQ Isolate, the Netherlands), Pea (PPI) was supplied by Yantai Shuangta Food Co., Ltd. (Pea Protein 85%, China) and Mung bean (MBPI) was provided by Fuji Oil (Fuji Oil MPI-ER, China). The protein content of the isolates was determined to be 78.9, 73.7 and 74.0% w/w for FBPI, PPI and MBPI respectively as measured using Dumas and a N-factor of 5.7. Fluorescent dyes Rhodamine B, NHS-Rhodamine, NHS-Fluorescein and SDS-PAGE supplies were purchased from Thermo Fisher Scientific (USA). All other chemicals (analytical grade) were from Merck (Germany). Demineralized water was used in all samples.

### 2.2. Powder milling

MBPI powder was found to give highly aerated dispersions at 15% w/w protein content. As such, it was subjected to a milling step before dispersion. This was done to decrease the powder particle size and airiness of the protein particles and improve powder dispersibility. A planetary bead mill (Pulverisette 5 Premium line, Fritsch, Germany) was used to mill MBPI for 8 1-min cycles at 400 rpm. Resting cycles of 1 min were included between every cycle to prevent the powder from heating as were 5-min resting cycles between cycles 3 and 4 and between cycles 6 and 7.

### 2.3. Sample preparation

Plant protein isolate was dispersed in demineralized water (15–16% w/w protein) and stirred by using an overhead stirrer for 2 h at room temperature. FBPI and PPI protein dispersions were homogenized by using a two-stage high pressure homogenizer (Panda Plus 2000; GEA, Italy) at 50 MPa (500 bar) for 2 cycles. During these 2 cycles, the temperature of the samples did not exceed 35 °C and afterwards protein content was adjusted to 15%. Sample preparation of PPI is visualized in Figs. SI-1. Fifteen percent MBPI protein dispersions could not be homogenized probably because the particles were too coarse or too hard. Therefore MBPI was diluted to 7.5% protein, homogenized (50 MPa, 2 cycles), freeze-dried and redispersed at 15% protein content. Both

homogenized and non-homogenized dispersions were adjusted to pH 7.0 by using 1M sulfuric acid/NaOH and standardized at an ionic strength of 30–45 mM NaCl equivalent.

Samples used for compression tests were prepared by pouring the 15% w/w protein dispersions into 10 mL syringes that were lubricated on the inside with a thin paraffin oil layer. The dispersions were then heated for 30 min at 95 °C in a water bath. The gels were cooled to room temperature for 1 h after which they were stored at 4 °C for at least 16 h. Before analysis, the gels were cut into cylinders 15 mm long and 15 mm in diameter and equilibrated to room temperature for 1 h.

#### 2.4. Dry matter dispersibility

The dispersibility of the different protein isolates in demineralized water at pH 7 was determined by centrifugation. Fifteen percent w/w protein dispersions were diluted to 5% w/w protein and then centrifuged at 4000g for 30 min (20 °C). The obtained supernatants and pellets were dried in an oven at 105 °C for a minimum of 16 h. The dry matter dispersibility was defined by the mass of dry matter in the supernatant divided by the initial mass of dry matter in dispersion.

#### 2.5. Particle size distribution

Static light scattering was used to determine the particle size distribution of (non) homogenized protein dispersions with a Mastersizer 3000 equipped with a wet sample dispersion unit (Malvern Instruments Ltd, UK). The measurements were conducted using a refractive index of 1.45 and 1.33 for the dispersed and continuous phase respectively and an adsorption index of 0.001. The particle size distribution was reported as volume based distribution and samples were measured in triplicate.

#### 2.6. SDS-PAGE

Non-reducing and reducing SDS-PAGE were conducted to analyse the protein composition of the different protein isolates. 4–12% Bis-Tris gels along with MES SDS running buffer were used. Protein dispersions were diluted to 0.1% protein content in pH 7.0 phosphate buffer and 15 µL was added to 45 µL of running buffer for non-reducing conditions. For reducing conditions, 6 µL of running buffer was replaced by 6 µL of DTT solution. All solutions were heated at 70 °C for 10 min and were then cooled down to room temperature and centrifuged (Hermle Z306, 1000g, 1 min). 15 µL of supernatant was loaded in each well and a molecular weight marker of 2.5–200 kDa (Mark12™, ThermoFisher) was loaded for reference. Electrophoresis was carried out at 200V for 35 min in a XCell Surelock Mini-Cell. Afterwards, the gels were washed with deionized water and stained using SimplyBlue SafeStain. The gels were stored in a 20% NaCl solution and scanned with a Bio-Rad GS900 gel scanner.

#### 2.7. Differential Scanning Calorimetry (DSC)

DSC was used to determine the denaturation temperatures of the different commercial protein isolates. High volume and Tzero Hermetic pans (TA Instruments, New Castle, USA) were filled with 15% w/w protein dispersion (pH 7). The samples were measured with a DSC25 differential scanning calorimeter (TA instruments, New Castle, USA) and heated from 20 to 120 °C with a temperature increase of 10 °C/min. All samples were measured in triplicate and data processing was performed with TRIOS software for thermal analysis from TA Instruments.

#### 2.8. Rheology

##### 2.8.1. Small amplitude oscillatory shear measurement

Gelation of protein dispersions (15% w/w protein, pH 7) was induced by performing a temperature sweep in a stress-controlled MCR302 rheometer (Anton Paar, Graz, Austria). The sample was

transferred into a sandblasted CC-17 concentric cylinder system. A layer of paraffin oil was placed on the sample and a solvent trap was used to prevent sample evaporation upon heating. During the temperature sweep, the samples were heated from 20 to 95 °C at a rate of 3 °C/min and the samples were maintained at 95 °C for 30 min. After that, the samples were cooled to 20°C at the same rate and lastly the sample was kept at 20 °C for 10 min to verify there was no further gel solidification. This test was performed at a fixed strain (0.1%) and frequency (1Hz), which did not exceed the linear viscoelastic regime (LVER). The viscoelastic response, storage modulus  $G'$  and loss modulus  $G''$ , were recorded throughout the measurement.

##### 2.8.2. Large amplitude oscillatory shear measurement

LAOS amplitude-sweep tests were performed to investigate the viscoelastic behaviour of protein gels in the non-linear viscoelastic regime. The heat-induced gels were subjected to an amplitude sweep from 0.01 to 1000% at a constant frequency of 1Hz and 20 °C.  $G'$  and  $G''$  were recorded as a function of strain. The critical strain of the heat set gels was defined to be the intercept of the constant plateau value  $G'$  in the linear-viscoelastic regime and the extrapolated slope during the steep decrease in  $G'$  at increasing strain (Figs. SI–2).

#### 2.9. Uniaxial compression test

The mechanical properties of gels were measured using a Texture Analyzer (TA.XT. plus, Stable Micro Systems Ltd, UK) equipped with a 1 or 5 kg load cell and P/50 (50 mm diameter) probe. An uniaxial compression test was performed at a compression speed of 1 mm/s up until 90% strain. Paraffin oil was applied on the probe and TA surface for lubrication. The engineering stress ( $\sigma$ ) of the gel was calculated by dividing the force (F) measured during compression by the initial cross-sectional surface area (A) of the gel ( $\sigma = F/A$ ). The engineering, Cauchy strain ( $\gamma$ ) was determined to be the change of gel height after compression ( $\Delta L$ ) divided by its initial height ( $L_0$ ) ( $\gamma = \Delta L/L_0$ ). The change in surface area during compression was not taken into account as gel samples deformed differently (Figs. SI–3). The stress and strain at the fracture point of the gels were studied, giving a measure for the hardness and brittleness, respectively. The Young's Modulus (E), which is equal to the slope of the linear part of the stress-strain curve ( $E = \Delta\sigma/\Delta\gamma$ ), was determined and is a measure of the stiffness of a gel. The measurements were performed at least in triplicate.

#### 2.10. Microscopy

##### 2.10.1. Single staining

Protein dispersions (15% w/w protein, pH 7, 30 mM) were labelled non-covalently with Rhodamine B having a final dye concentration of 0.005%. The stained dispersions were transferred to sealed glass slides (Gene frame 65 µL adhesives, Thermo Fisher Scientific, UK) and heated in a water bath at 95 °C for 30 min after which they were cooled down to room temperature.

##### 2.10.2. Double staining

Two different fluorescent dyes were used to covalently label the dispersible and insoluble fraction of the plant protein isolates to distinguish their separate orientation in the microstructure. Fifteen percent w/w protein dispersions were diluted to 5% w/w protein with demineralized water and centrifuged as described in Section 2.4. The pellet (referred to as insoluble fraction) and supernatant (referred to as dispersible fraction) were incubated at pH 7.0 for 1 h (20 °C) with NHS-Fluorescein and NHS-Rhodamine respectively, at a concentration of 167 ppm w/w protein. The dispersible fraction was dialyzed using dialysis membranes with 12–14 kDa pore size for ~24h at 4 °C including 3 water refreshments. The insoluble fraction was washed and centrifuged 4–5 times (4000g, 30 min) until the supernatant was colourless. Both

fractions were freeze-dried and redispersed in demineralized water and stirred for 2 h at room temperature. Insoluble and dispersible fractions were combined for a final protein concentration of 12–15% w/w and stirred for 1 h. Microscope slides were prepared and heated as described in the previous section.

The microstructures were visualized using a Nikon C2 confocal laser scanning microscope. A 10× objective and 60× oil immersion objective were used for magnification. For (NHS-)Rhodamine B labelled protein samples, the laser excitation wavelength was 561 nm and the emitted signal was acquired with a 595/40 nm filter. Additionally for the double stained samples, NHS-Fluorescein was excited at 488 nm and the emitted signal was detected using a 525/50 nm filter.

### 2.11. Statistical analysis

Measurements were conducted at least in duplicate with at least two prepared samples, except for SDS-PAGE and CLSM analysis. Unless stated otherwise, all results are presented as mean  $\pm$  standard deviation. Significant differences between sample treatments (stirred vs stirred + homogenized) and among the three protein isolates were determined by a one-way analysis of variance (ANOVA) followed by a Duncan post hoc test. A significance level of  $p < 0.05$  was used and analysis was conducted with SPSS Version 28 (IBM Corp., USA).

## 3. Results

Fig. 1 shows a schematic overview of our study. As mentioned, three distinct commercial plant protein sources were studied that cover a broad range of degrees of dispersibility and a broad range of fractions of insoluble particles, with commercial fava bean protein isolate (FBPI)

having the highest dispersibility and smallest fraction of insoluble particles, commercial mung bean protein isolate (MBPI) having the lowest dispersibility and largest fraction of insoluble particles, and commercial pea protein isolate (PPI) being intermediate. As representative mild agitation we use an overhead stirrer ('Stirred' samples). Part of the stirred samples were additionally homogenized. Both the stirred and stirred + homogenized samples were analysed using a range of methods, as we describe below.

### 3.1. Effect of homogenization on protein dispersion

First, consider the impact of homogenization on the particle size distribution of the protein dispersions. Homogenization reduced the particle size in all cases, but the effect was largest for FBPI followed by PPI and MBPI (Fig. 2). This indicated that the mechanical forces during homogenization broke down and dissociated commercial plant protein particles and that the extent was different per source. As observed with light microscopy (results not shown) FBPI contained less insoluble particles ( $>50 \mu\text{m}$ ) compared to PPI and MBPI, and these were all broken down into smaller particles under the homogenization conditions used here. We observed that concentrated dispersions (15% w/w protein) of MBPI could not be homogenized. This could possibly be due to hard and coarse particles. These results are in line with earlier work, which also established a decrease in particle size by homogenization treatment. For example, this was established for commercial pea proteins (Luo, Wang, et al., 2022; Ong et al., 2022), lentil proteins (Saricaoglu, 2020), novel fruit seed and hemp seed proteins (Zhao et al., 2023), commercial chickpea protein (Huang et al., 2022), lupin protein (Bader et al., 2011), 11S soy protein (Kang et al., 2022) and fava bean proteins (Yang et al., 2018). Our results however, by comparing multiple

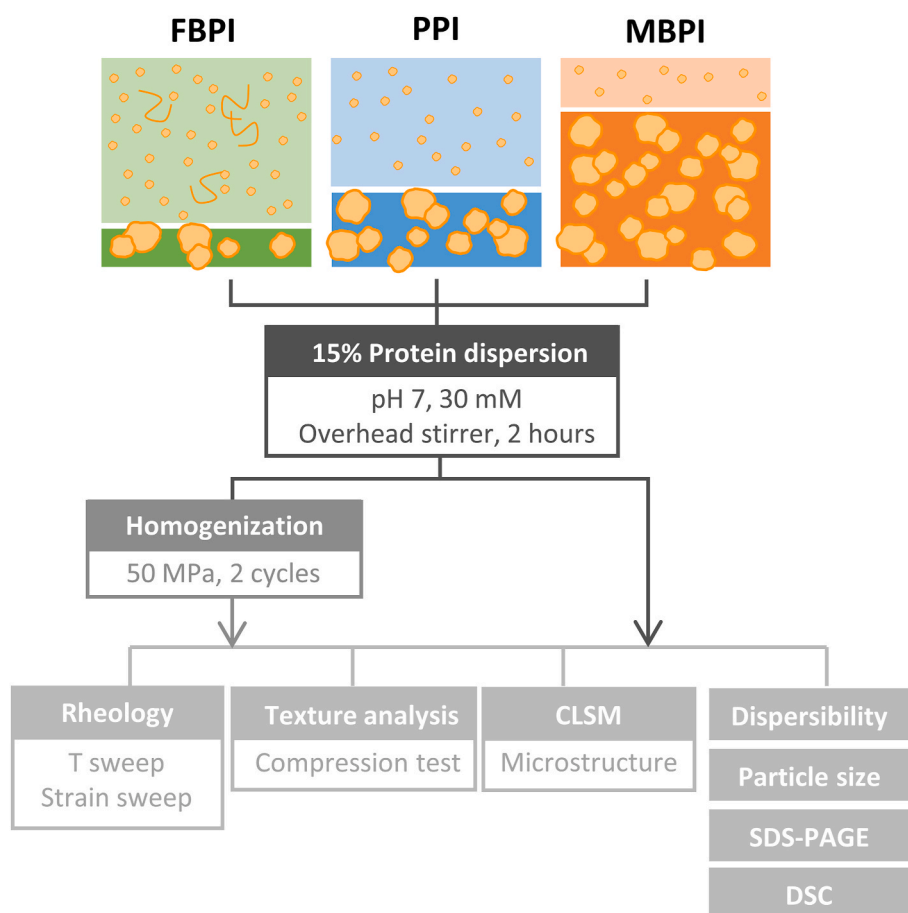
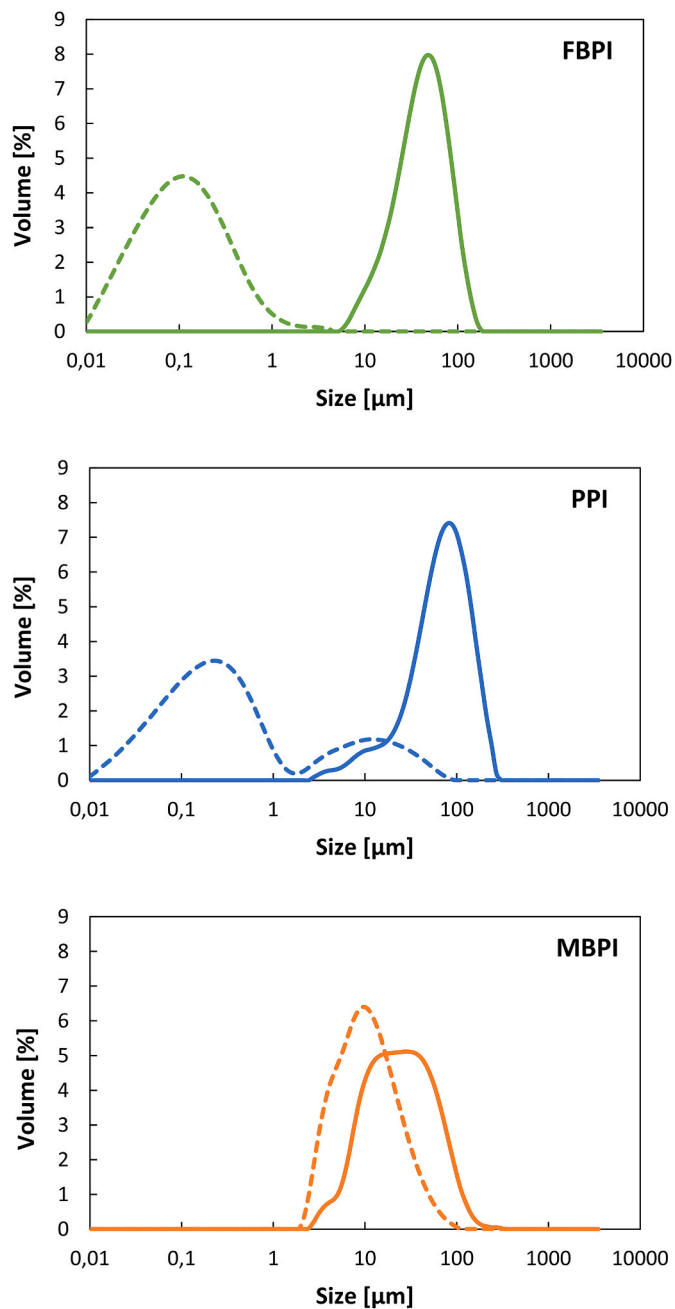


Fig. 1. Schematic overview of plant protein model systems, treatment and analysis. Plant proteins were dispersed, stirred and either homogenized or not.





**Fig. 2.** Particle size distribution decreased after homogenization of FBPI (green), PPI (blue) and MBPI (orange) dispersions. Stirred samples are indicated by a solid line and stirred + homogenized samples are indicated by a dashed line.

sources, clearly demonstrate that the extent to which particles can be broken down under identical homogenization conditions, is very much source-dependent.

The particle size distributions do not yet inform about the fraction of material that is present as insoluble particles. Therefore, the fraction of dispersible material ('dispersibility' in %), both before and after homogenization was determined. Fig. 3 shows that FBPI had the highest dispersibility whereas PPI and MBPI were significantly less dispersible ( $p < 0.05$ ) without treatment. This may indicate that the three protein isolates were produced using different processing conditions which affected the protein particles' state and size. Homogenization positively affected dispersibility for all sources, but clearly, the least dispersible protein isolates (PPI and MBPI) benefited most from the homogenization

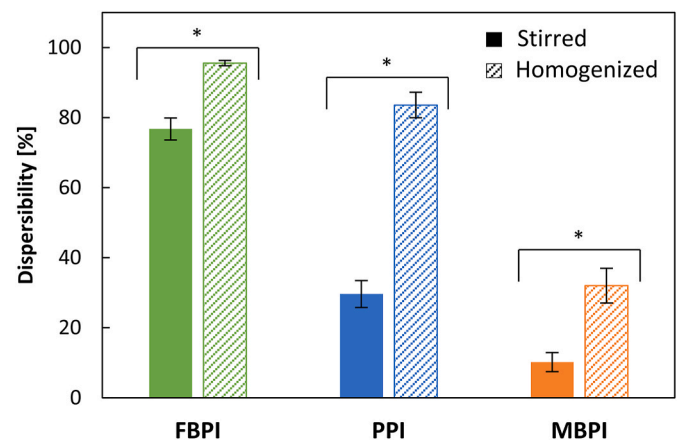


**Fig. 3.** Dry matter (DM) dispersibility of the protein dispersions increased after homogenization. Stirred samples are indicated by a solid bar and stirred + homogenized samples by a dashed bar. Dry matter dispersibility is defined as the percentage of DM that remained in the supernatant after centrifugation at pH 7. Asterisk \* indicates a significant difference ( $p < 0.05$ ) between treatments.

treatment. Again, these findings are in line with earlier studies on pea proteins (Luo, Wang, et al., 2022; Ong et al., 2022), lentil proteins (Saricaoglu, 2020), novel fruit seed and hemp seed proteins (Zhao et al., 2023), commercial chickpea protein (Huang et al., 2022), lupin protein (Bader et al., 2011), 11S soy protein (Kang et al., 2022) and fava bean proteins (Yang et al., 2018).

Note however, that while we use a single homogenization condition for all three sources (50 MPa, 2 cycles), in general the relation between homogenization pressure, cycles and protein dispersibility seems to have a source-dependent optimum, as reported by Saricaoglu and Kang (Kang et al., 2022; Saricaoglu, 2020). As mentioned earlier, during homogenization proteins can unfold due to mechanical forces and thermal effects, which may lead to protein re-aggregation and an increase in particle size. Possibly for example, the MBPI might benefit from treatment at higher pressures with more cycles, whereas for FBPI more extensive treatment may not be needed or may even have adverse effects.

### 3.2. Gelling behaviour after homogenization

#### 3.2.1. Small deformation rheology

While for food functionality it is mainly the non-linear, large deformation rheology that is of importance, the linear small deformation rheology is useful as a first characterization method, that is often more amenable to theoretical interpretation. Additionally, linear rheology analysis can give insight into gel property development during the total gelation process. Fig. 4A shows a representative measurement of the development of the storage modulus  $G'$  and loss modulus  $G''$  during heating and subsequent cooling of the protein dispersions. Fig. 4B reports values of the modulus  $G'$  at key time points for the three protein sources, for both stirred and stirred + homogenized samples during the temperature sweep.

Normally, during heat-induced gelation, a gel point is defined as the point of the transition from  $G' < G''$  to  $G' > G''$  and this is a widely accepted criterion for the transition of a viscous material into a viscoelastic gel. In our study, only FBPI samples showed this point after ~13 min at ~59 °C, regardless of the treatment. All other samples already showed  $G' > G''$  from the beginning of the temperature sweep, although the unheated protein dispersions were no gels. It should be noted that there was a difference in  $G'$  and  $\tan \delta$  ( $\tan \delta = G''/G'$ ) at 20 °C between stirred and stirred + homogenized PPI, which is in accordance with the liquid-like state of the stirred sample ( $G' \sim 1\text{--}10$  Pa,  $\tan \delta = 0,8$ ) and the more pasty state of the stirred + homogenized sample ( $G' \sim 100$  Pa,  $\tan \delta = 0,3$ ).

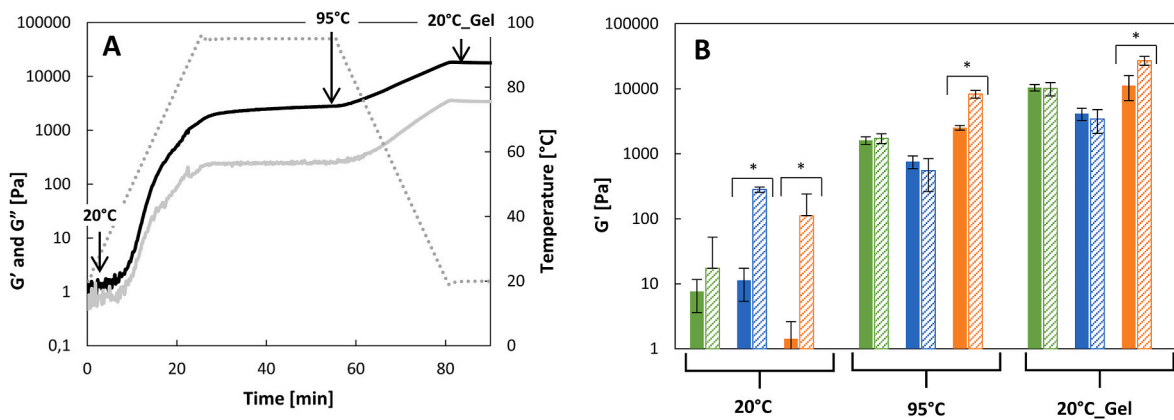


**Fig. 4.** A) Example of storage modulus  $G'$  (solid black line) and loss modulus  $G''$  (solid grey line) development during a temperature sweep (dotted grey line) in rheometer on a 15% w/w plant protein dispersion at pH 7. Arrows indicate temperatures at which  $G'$  values are compared in Figure B. B)  $G'$  of 15% w/w FBPI (green), PPI (blue) and MBPI (orange) stirred protein dispersions (solid bar) and stirred + homogenized dispersions (dashed bar) at 20 °C, 95 °C and 20 °C after temperature sweep. Asterisk \* indicates a significant difference ( $p < 0.05$ ) between treatments.

During heating, the modulus  $G'$  of all samples increased as a result of mainly hydrophobic interactions and to a lesser extent covalent bonds. As often observed, upon cooling the moduli increase was further enhanced, possibly due to electrostatic interactions and the formation of hydrogen bonds (Tanger, Müller, Andlinger, & Kulozik, 2022). Final moduli  $G'$  after cooling were around  $10^3$ – $10^4$  Pa. The highest modulus for stirred samples was observed for MBPI ( $11 \pm 4.7$  kPa), followed by FBPI ( $10 \pm 1.2$  kPa) and PPI ( $4.1 \pm 0.8$  kPa). Interestingly, particle size reduction through homogenization only increased  $G'$  for MBPI (to  $27 \pm 4.2$  kPa) ( $p < 0.05$ ) and did not affect the final linear storage moduli of the other heat-induced gels ( $10 \pm 2.3$  kPa for FBPI and  $3.4 \pm 1.3$  kPa for PPI). After the temperature sweep, a frequency sweep was performed (at 0.1% strain) and there we observed similar behaviour for all samples regardless of source or treatment. We found that  $G' > G''$  over the whole tested frequency range and  $G'$  only slightly increased at increasing frequency, which indicates the viscoelasticity of the gels (example in Figs. SI-4).

Our findings are in contrast with some earlier work on homogenized lab-extracted proteins. An increase in  $G'$  from  $\sim 1100$  to  $\sim 3000$  Pa was found for a heat-induced 9% soy protein gel after homogenization (150 MPa, 2 cycles) (Kang et al., 2022). In another study,  $G'$  for a 5% quinoa heated dispersion doubled after homogenization (50 MPa, 5 cycles) although these structures were only very weak gels ( $G \sim 10^1$  Pa) (Luo, Cheng, et al., 2022). These authors found that the effect on  $G'$  was proportional to the homogenization pressure and number of cycles, but the used conditions were not comparable to our study, since dilute systems containing lab-extracted proteins were used.

Additionally, the effect of homogenization may depend on the protein source. Indeed, again for lab-extracted proteins, Zhao (Zhao et al., 2023) showed an increase in  $G'$  of homogenized heat-induced gels varying from  $\sim 10^2$  to  $10^5$  Pa depending on the (novel) protein source. However, in other cases, such as for plum seed protein isolate, homogenization did not have an impact on  $G'$ .

A final comparison is with a lab-extracted unhomogenized FBPI. For samples heated under comparable conditions, a  $G'$  of approximately 2 kPa was found (Langton et al., 2020), a considerably lower value than in our experiment. Because of their use of lab-extracted proteins, all of these results may not be directly comparable to our reported results, since in our case the proteins may already be substantially denatured and contain significant fractions of insoluble particles. Kornet reported a  $G'$  of about  $\sim 1$ – $5$  kPa for a 15% commercial PPI gel and pea protein lab-extracted by isoelectric precipitation, but for pea protein lab-extracted by diafiltration this  $G'$  value about doubled (Kornet et al., 2021).

In a rare example of a report on commercial pea protein isolate (Ong

et al., 2022), stirred protein dispersion (15% w/w protein) could not form a heat-induced gel in contrast to homogenized dispersions. These gels were still rather soft and had a  $G'$  of  $\sim 10^3$  Pa, independent of pressure (60–120 MPa) and number of cycles (1–3). However, when increasing the number of cycles to 5 or increasing the pressure to 180 MPa for at least 3 cycles, the  $G'$  was significantly increased.

### 3.2.2. Large deformation rheology

The results of our non-linear rheological characterization of the different protein gels under oscillatory shear deformation are shown in Fig. 5. Representative flow curves (shear modulus  $G'$  versus strain at a fixed frequency of 1 Hz) are presented in Fig. 5A. The gels did not show clear fracture but rather exhibited a broad regime of plastic deformation. As a measure of their deformability, we determined the critical strain demarcating the end of the linear viscoelastic region and the start of the non-linear viscoelastic region of plastic deformation. Homogenization only increased the critical strain of FBPI, promoting the deformability of the gel. The critical strain and thus deformability of the MBPI gels was found to be remarkably low as compared to the FBPI and MBPI gels ( $p < 0.05$ ). We found that the critical strain correlated with the fraction of insoluble particles in the protein isolates: MBPI produced brittle gels whereas PPI and FBPI produced more ductile gels.

### 3.2.3. Compression test

Especially for non-linear deformations, mechanical behaviour may depend on the type of deformation. Compression is a type of deformation that is highly relevant for foods, hence we also used a compression test to characterize the complementary mechanics of our heat-induced gels. Fig. 6 shows representative stress-strain curves under compression for FBPI, PPI and MBPI heat-induced gels obtained from stirred and stirred + homogenized protein dispersions. These curves show the same significant effect of homogenization for all three sources: the gels reach higher stresses and strains before failing, and if they fail they do so in a more brittle manner than the gels obtained from the stirred dispersions; these fail in a more ductile manner. Unhomogenized PPI and MBPI showed very weak gelation ability, and the structures formed after heating showed more yielding than fracture. Concerning differences between the sources, it is clear that the isolate with the highest dispersibility and smallest fraction of insoluble particles produced the strongest gels: the FBPI gels obtained from only stirred dispersions and stirred + homogenized dispersions reached the highest stresses and largest deformations before failing. On the other hand, changes due to homogenization, especially at lower strains, were large for the source that was least dispersible and which had the largest fraction of insoluble particles (MBPI).

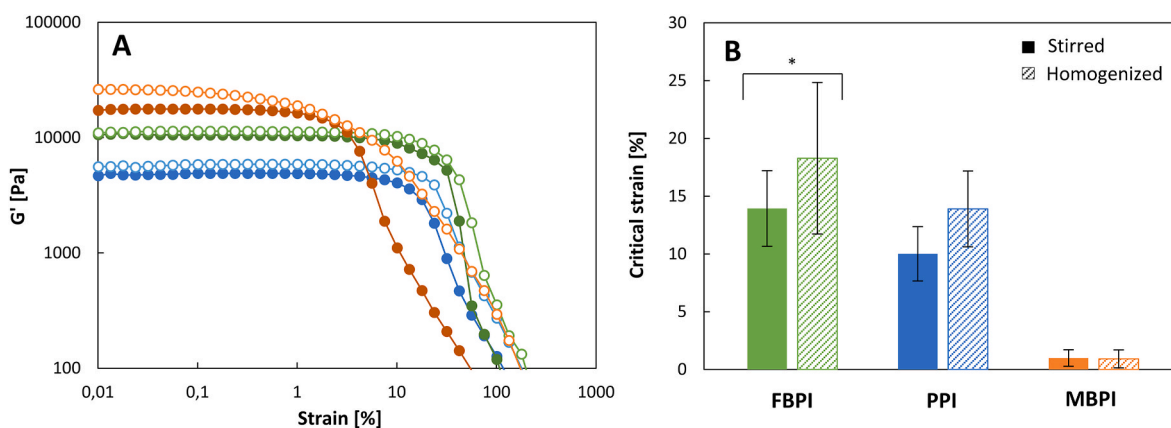


**Fig. 5.** (A) Amplitude sweep of 15% w/w FBPI (green), PPI (blue) and MBPI (orange) heat-induced gels. Stirred samples are indicated by filled circles and stirred + homogenized samples by open circles. The critical strain of the gels (B) was defined to be the intercept of the constant plateau value  $G'$  in the linear viscoelastic regime and the extrapolated slope during the steep decrease in  $G'$  at increasing strain. Asterisk \* indicates a significant difference ( $p < 0.05$ ) between treatments.

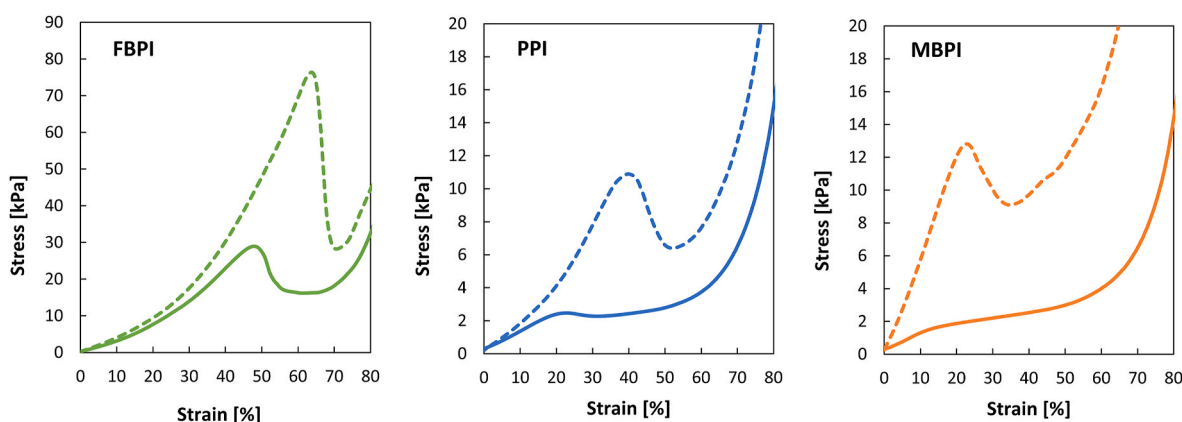


**Fig. 6.** Stress-strain curves of stirred (solid line) and stirred + homogenized (dashed line) heat-induced FBPI (green), PPI (blue) and MBPI (orange) gels (15% w/w protein, pH 7) obtained during uniaxial compression. Note that FBPI stress axis  $\gg$  PPI and MBPI stress axis.

From the initial linear slopes of the compression curves, the estimate of the Young's modulus was derived for each source, which is shown in Fig. 7. Homogenized gels showed an increase in stiffness, but this effect was most pronounced for MBPI. For incompressible samples (Poisson's ratio  $\mu = 0.5$ ) the Young's modulus  $E$  is expected to be related to the

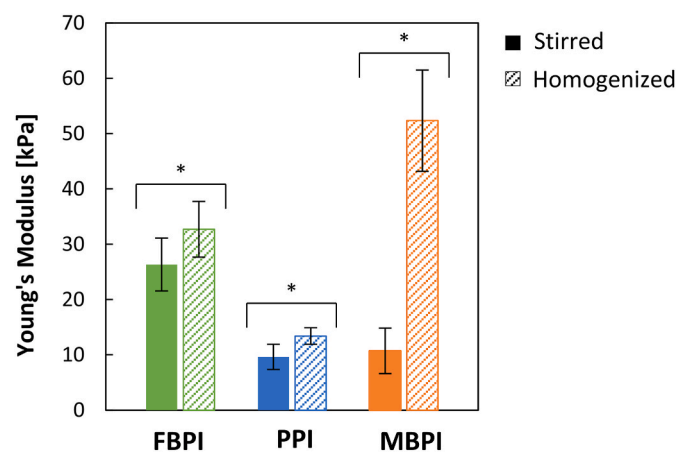


**Fig. 7.** Young's modulus of heat-induced FBPI, PPI and MBPI gels (15% w/w protein, pH 7) obtained during uniaxial compression. Solid bars indicate stirred dispersions and dashed bars indicate stirred + homogenized dispersions. Asterisk \* indicates a significant difference ( $p < 0.05$ ) between treatments.

(zero frequency) shear modulus  $G$  by  $E \sim 3G$ , as both  $G$  and  $E$  are measured in the linear deformation regime (Mezger, 2014; Stading & Hermansson, 1991). For all FBPI samples and PPI samples, this correlation indeed holds to a reasonable approximation (ratio  $E:G \sim 2.3\text{--}3.9$ ; assuming that  $G'$  at 1Hz is close to  $G$ ) (Table SI-1). In addition,  $E$  followed the same order of magnitude as  $G$  for homogenized samples;  $MBPI > FBPI > PPI$ . However, especially for stirred MBPI samples there appears to be a discrepancy between the moduli found in shear and compression. Since the breaking strain of stirred MBPI (Fig. 5) is very low, we in fact assume that these gels already fail at very low strains in the compression test, limiting our ability to reliably determine  $E$  for this case.

### 3.3. Microstructure

To be able to relate the mechanical behaviour to the microstructure of the heat-induced protein gels, CLSM was used to visualize gel structures at the  $\mu\text{m}$  scale. First, the non-covalent dye Rhodamine B was used to visualize the entire heat-induced gel protein network. We did this for samples of which the proteins were dispersed by only stirring ("stirred"), and for samples for which the proteins were dispersed by both stirring and homogenization ("stirred + homogenized") (Fig. 8).

For the stirred samples, the images of the PPI and MBPI gels show a microstructure of quite densely packed insoluble particles in a continuous matrix. From the images for FBPI the fraction of these insoluble particles appeared lower, and the extent of the continuous matrix



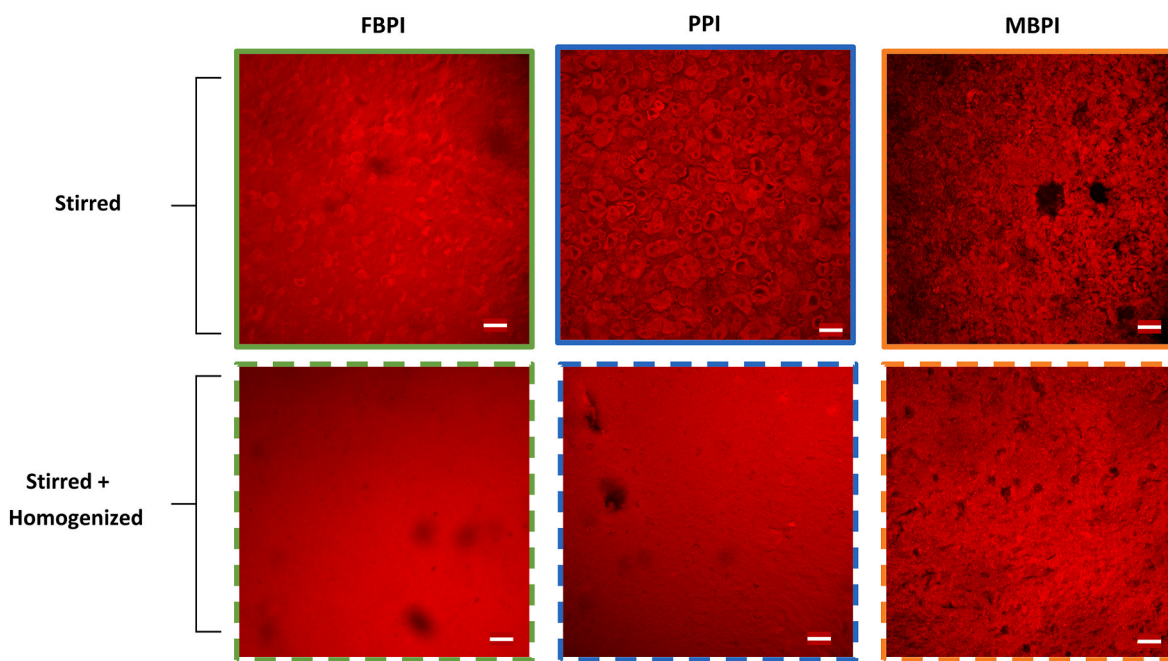


**Fig. 8.** CLSM images visualizing the microstructure of heat-induced gels of stirred (upper row) and stirred + homogenized (lower row) FBPI (green), PPI (blue) and MBPI (orange) dispersions (15% w/w protein, pH 7). Proteins are shown in red and the scale bar indicates 100  $\mu\text{m}$ .

appeared to be larger than for PPI and MBPI gels.

Upon homogenization, the particle size of the protein dispersions decreased and this also led to a more homogeneous microstructure, especially for FBPI and PPI. Homogenized MBPI had a less fine gel microstructure, possibly due to freeze drying and re-dispersion after homogenization before gelation.

Large, polydisperse irregularly shaped insoluble particles were also observed in microscopy images of heat-induced gels made from commercial PPI (Johansson et al., 2021; Kornet et al., 2021) and in enzyme crosslinked commercial soy protein isolate gel (Herz, Schäfer, Terjung,

Gibis, & Weiss, 2021). On the other hand, in the study of Ben-Harb (Ben-Harb et al., 2018), a more homogeneous appearance of a commercial PPI gel was observed after heating. Above all, it was clear that the microstructure of heat-induced gels obtained from commercial plant protein powders was remarkably different than that for similar proteins isolated at lab scale. The microstructure of lab-extracted PPI (Kornet et al., 2021), FBPI (Langton et al., 2020), quinoa protein isolate (Luo, Cheng, et al., 2022) and soy protein isolate (Ersch et al., 2016) was smoother and more homogeneous than our gels.

Next, we aimed at separately imaging the fraction of the proteins that

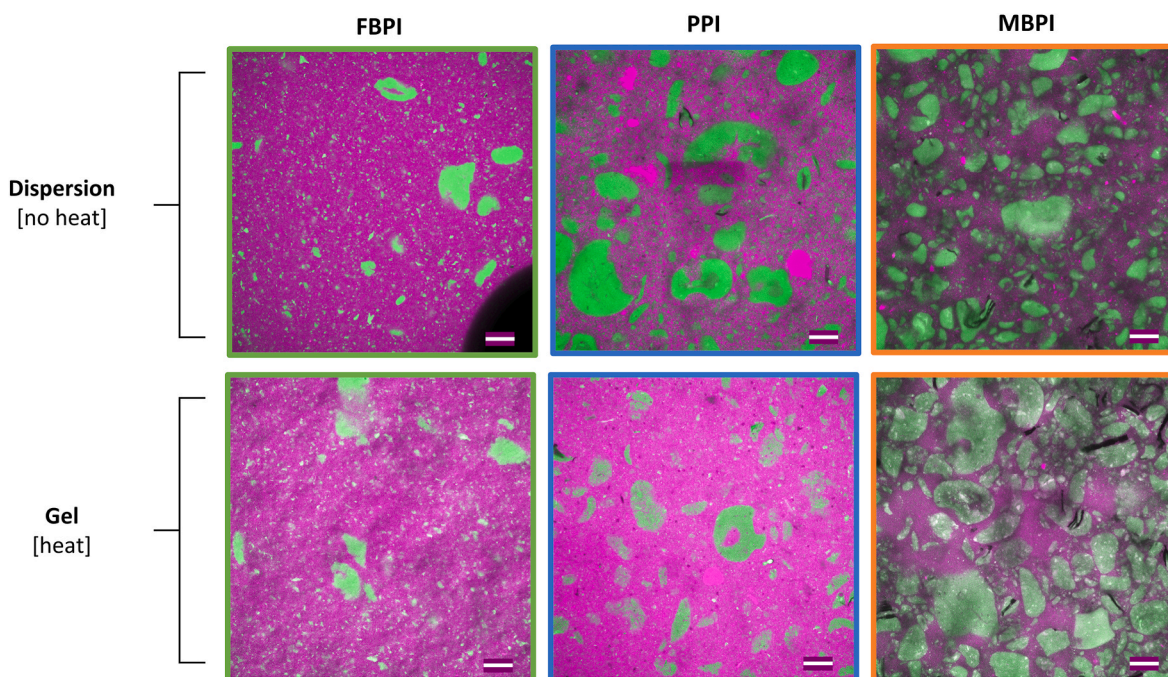


**Fig. 9.** CLSM images visualizing the insoluble fraction (green) and dispersible fraction (magenta) of FBPI (green), PPI (blue) and MBPI (orange) stirred dispersions (upper row) and heat-induced gels (lower row) (12–15% w/w protein, pH 7). The scale bar indicates 20  $\mu\text{m}$  and intensities are not quantitative.



was initially well-dispersed (“dispersible fraction”) and the fraction that was initially poorly dispersed (“insoluble fraction”). To do so, we separated the dispersible fraction and insoluble fractions by centrifugation and covalently conjugated different fluorescent dyes to the two different fractions. After thoroughly removing all free dye, the two fractions were recombined and heated to form gels. Results are shown in Fig. 9. It was observed that the initially insoluble particles (green) remained visible after heating and were homogeneously distributed throughout a continuous network consisting of the initially dispersible proteins (magenta) (Fig. 9).

### 3.4. Characterization of protein isolates

The difference that we observe in terms of microstructure and mechanical properties for FBPI, PPI and MBPI may not only be due to differences in dispersibility and the fractions and size distributions of insoluble particles. At least in part they probably also arise as a consequence of the different nature of the proteins in the different seeds. To address this, we performed additional characterization experiments on the three different protein powders and dispersions.

SDS-PAGE analysis was performed to determine the protein fractions in each protein isolate, as can be seen in Fig. 10. FBPI and PPI contained both legumin (11S) and vicilin (7S/8S) fractions whereas MBPI consisted mainly of vicilin. In FBPI and PPI, Legumin is the major component (~60 kDa) which can be dissociated into a ~40 kDa  $\alpha$ -legumin and ~20 kDa  $\beta$ -legumin under reducing conditions as these subunits are covalently linked by disulphide bonds. Other bands indicated Convicilin (~70 kDa) and Vicilin (~33 and 50 kDa) (FBPI (Sharan et al., 2021; Vogelsang-O'Dwyer et al., 2020; Warsame, Michael, O'Sullivan, & Tosi, 2020); PPI; (Kornet et al., 2021; Moll et al., 2022)). The bands at 26, 30, and 50 kDa in the MBPI lane indicated the presence of various vicilin subunits (Amaral, Ferreira, Silva, Neves, & Demonte, 2017; Tang & Sun, 2010; Yang, Eikelboom, van der Linden, de Vries, & Venema, 2022). Note that part of the proteins were not able to enter the gel, indicated as large/insoluble material in the figure. This means that these commercial plant protein isolates contain at least some material that is resistant to

dissolution even in the presence of SDS and a reducing agent. Homogenization of samples did not lead to changes in the protein composition, as observed in SDS-PAGE (Figs. SI-5). This was also found in other studies that used homogenization (Baskinci & Gul, 2023; Keuleyan et al., 2023; Luo, Cheng, et al., 2022; Ma, Zhang, He, Xu, & Guo, 2023; Saricaoglu et al., 2018) except in the study of Luo (Luo, Wang, et al., 2022), where the disulfide bond in pea legumin seemed to be broken up after homogenization (50 MPa, 3 cycles). In addition, it should be noted that the protein composition was different between the total dispersion and dispersible fraction (proteins in supernatant after centrifugation) of stirred PPI and MBPI (Figs. SI-6). Slight differences were also observed for commercial PPI in other studies (Keuleyan et al., 2023; Moll et al., 2022).

Since different proteins may have different functional properties, compositional differences may also lead to functional differences. First, when comparing the gelation properties of different protein fractions within the same source, it has been reported that soy glycinin [11S] makes stiffer, harder and more deformable gels than  $\beta$ -conglycinin [7S] (Renkema, Knabben, & Van Vliet, 2001). In addition, Fava bean legumin [11S] produced gel with a higher  $G'$  than its vicilin [7S] component at low ionic strength (Johansson, Karkehabadi, Johansson, & Langton, 2023). In contrast, for pea protein mainly vicilin [7S] contributes to heat-induced gelation as only legumin [11S] could not form a heat-induced gel in the study of Bora (BORA et al., 1994). Second, we can also compare the gelation properties of proteins that have similar composition but come from a different source. In the study of Ge (Ge et al., 2023), the gelation properties of various legume proteins were reported and it was found that the hardest heat-induced gels were formed by sources that contained phaseolin, a type of vicilin [7S]. However, other sources consisting of mainly vicilin produced weak gels. So, from the current literature we can state that there is no clear correlation between the main protein fractions [11S and 7S] and gelation properties across legume species.

DSC was performed to assess to which extent the proteins in the different isolates had retained their native configuration. Results are shown in Table 1 and DSC thermograms can be found in Figs. SI-7. A

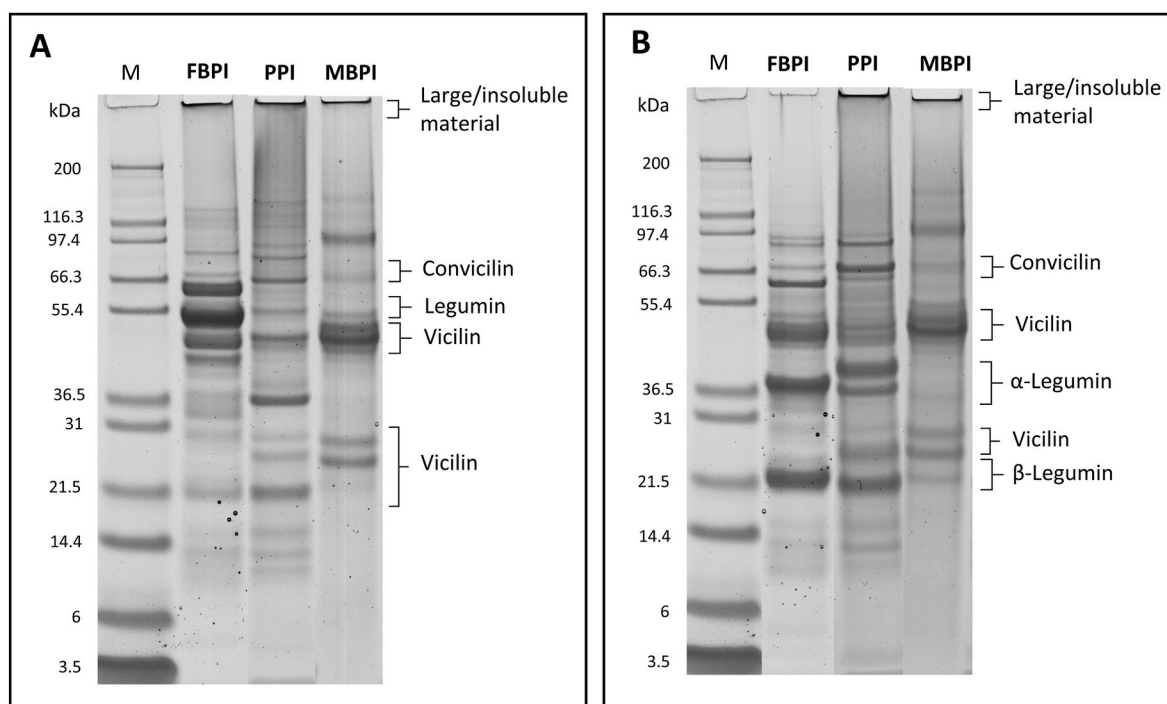


Fig. 10. SDS-PAGE profile of FBPI, PPI and MBPI under non-reducing (A) and reducing conditions (B). A molecular weight marker is included (M) and corresponding molecular weights are indicated on the outer lanes.

**Table 1**

Thermal characteristics including denaturation onset temperature ( $T_{\text{onset}}$ ), denaturation peak temperature ( $T_d$ ) and endothermic heat enthalpies ( $\Delta H_d$ ) of 15% w/w protein dispersions. Samples were heated from 20 to 120 °C and measured in triplicate. Standard deviations are shown in superscript.

Protein source	$T_{\text{onset}}$ (°C)	$T_d$ (°C)	$\Delta H_d$ (J/g)
FBPI	84,4 <sup>±0,41</sup>	95,6 <sup>±0,27</sup>	1,38 <sup>±0,06</sup>
PPI	–	–	–
MBPI	–	–	–

denaturation peak was only found for FBPI, indicating that this powder at least still contained a fraction of some native proteins. The onset temperature for denaturation of 84 °C and peak denaturation temperature of 96 °C are in agreement with earlier results of Nivala (Nivala, Mäkinen, Kruus, Nordlund, & Ercili-Cura, 2017). But the endothermic heat enthalpy of their FBPI was significantly higher (~11,5 J/g); possibly the result of the milder protein production process. We could not distinguish separate peak temperatures in the thermogram, while Yang (J. Yang et al., 2018) reported separate denaturation temperatures for the vicilin (89 °C) and legumin fraction (105 °C). In any case, we observed that homogenization did not impact the DSC results for FBPI (Figs. SI-7 and Table SI-2).

Next to these protein properties, other studies also focused on the effect of homogenization on more molecular properties such as hydrophobicity, zeta-potential and the proteins' secondary structure. However, in our study, additional molecular analysis was limited as most of these tests require soluble material to produce reliable and consistent results. Since we deal with insoluble, large and heterogeneous starting material, we were bound to analysis on powder for further understanding. According to the FT-IR spectra, the secondary protein structure was rather insensitive to homogenization treatment (Figs. SI-8). The absorbance patterns were similar and peaks in the second derivative figure overlapped. This is in line with the findings of Luo, Cheng, et al. (2022) for homogenized quinoa protein isolate, and another study found only limited impact of on the secondary structure of pea proteins in the supernatant homogenization after homogenization (Luo, Wang, et al., 2022).

#### 4. Discussion

We will discuss our main findings on the impact of the insoluble particles on the heat-gelation of industrial plant protein isolates, in the broader context of the current literature. But first, we briefly discuss some practical problems we encountered when homogenizing commercial plant protein isolates, which are also important during industrial processing.

The first problem is air entrapment in concentrated protein dispersions. This mostly occurs during the initial dispersion stage, and may have significant consequences during further processing. Indeed, we observed air was included during stirring (visible for FPBI) and air bubbles were observed after heat-induced gelation in all sources (Figs. 8 and 9). In other studies, microscopic images of dense protein gels were also found to have air in the system (Herz et al., 2021; Kornet et al., 2021). Air bubbles can cause deviations in rheological measurements and texture analysis. For example, when measuring shear moduli during heating and cooling, the bubbles will expand and contract, and this may affect the measurements. Alternatively, like solid particles, air bubbles may be points of nucleation during fracture.

Indeed, we found that a mild centrifugation step quite affected gel properties in compression testing and rheological analysis (see results for FBPI in Figs. SI-9). In our study, we have taken precautions so that the impact of air bubbles was minor as compared to the effects of the insoluble particles in the protein isolates. However, we hypothesize that in an industrial setting, if not controlled properly, air bubbles may significantly affect the mechanical properties of any heat-induced gels

formed during processing.

We also observed that efficient homogenization is often impeded by the high viscosities of the starting dispersions, and repeated homogenizations can be difficult since homogenization itself can also lead to strong increases in viscosity and even the formation of viscoelastic dispersions.

Hence, from a practical point of view, it should be noted that the presence of air, high viscosity and hard particles in protein dispersion can be limiting factors in homogenization. Therefore, each commercial protein will require a tailored homogenization process to shape its functionality and this may include pre-treatment such as centrifugation, dilution or high shear mixing.

Next, we turn to the main conclusions we obtained from our research on the impact of insoluble particles on the heat-gelation of industrial plant protein isolates. A first, more or less obvious finding is that we conclude that homogenization decreased the particle size and insoluble fraction of plant protein dispersions. This is of course fully in line with the findings of other researchers for both commercial protein isolates (Burger, Singh, Mayfield, Baumert, & Zhang, 2022; Huang et al., 2022; Keuleyan et al., 2023; Moll, Salminen, Schmitt, & Weiss, 2021; Ong et al., 2022; Sun et al., 2022; Tang, Wang, Yang, & Li, 2009) and lab-extracted proteins (Baskinci & Gul, 2023; Kang et al., 2022; Luo, Cheng, et al., 2022; Ma et al., 2023; Saricaoglu, 2020; Saricaoglu et al., 2018; Yang et al., 2018; Zhao et al., 2023) though the extent differs per protein source, homogenization pressure and number of cycles.

However, most of these studies consider homogenization of diluted protein dispersions with protein contents between 2 and 10% w/w. These concentrations are typically too low for industrial plant protein isolates to be directly used in heat-induced gelation. Only in one study a 20% w/w dry matter dispersion was homogenized, but in this study the proteins were freeze-dried to allow more convenient analysis (Huang et al., 2022). Such additional drying steps are common in academic studies but may lead to additional protein aggregation and challenges during redispersion. Therefore, when the aim is to understand the impact of homogenization alone, we should aim to directly use homogenized dispersions, when possible.

Earlier work on plant protein gels has generally shown moderate to high increases of storage moduli  $G'$  due to homogenization of the protein dispersion (Baskinci & Gul, 2023; Luo, Cheng, et al., 2022; Ong et al., 2022; Saricaoglu, 2020; Zhao et al., 2023). In our study, we found that the storage modulus  $G'$  and breaking shear strain of heat-induced commercial plant gels were not systematically impacted by homogenization, as only one out of three protein dispersions showed an in these parameters. We wish to emphasize however, that the linear viscoelastic moduli are not particularly relevant in food processing and for food texture, and that large-deformation behaviour should always be taken into account as well.

Until now, there is only one study that performed large deformation rheology on homogenized heat-induced protein gels (Luo, Cheng, et al., 2022). Moreover, there are only two studies that use a texture analyser to determine the mechanical properties (Bader et al., 2011; Kang et al., 2022) of which one study also used small deformation rheology. However, none of them studies a system that is comparable to ours, involving dense commercial protein isolate dispersions that were homogenized at moderate pressure and directly used for heat-induced gelation (except for MBPI).

Indeed, the fracture properties of a gel strongly depend on the defects and inhomogeneities present (Foegeding, Bowland, & Hardin, 1995; van Vliet, 1996; Van Vliet & Walstra, 1995). We hypothesize that the key effect of homogenization was to improve the homogeneity of the gels, making them less susceptible to fracture upon compression. A possible mechanism could be that by improving the dispersibility of the protein particles, we have increased the availability for molecular protein-protein interactions driving gelation. We assume the nature of these interactions is the same as those identified for general heat-induced (plant) protein aggregation: hydrophobic- and

electrostatic interactions, as well as hydrogen bonds. After homogenization a larger fraction of proteins will be involved in (continuous) gel network formation, and the volume fraction and size of insoluble particles that disturb the network is smaller.

## 5. Conclusion

In this work, we showed that decreasing the insoluble fraction of three commercial plant protein isolates by homogenization yielded heat-induced protein gels with improved resistance to fracture upon compression. At the same time, shear deformation properties were not consistently impacted by homogenization. We hypothesize that without treatment, insoluble particles remain inert upon heating, and act as defects in the structure, contributing to the generally poor fracture properties of commercial plant proteins. After homogenization particles are smaller, allowing more network interaction and delaying fracture initiation. Although other studies already showed the effectiveness of homogenization as a tool to break up particles and increase dispersible matter, we found that treatment parameters and outcomes depended on the isolate properties. Even for FBPI, which still contained native proteins and had the highest fraction of dispersible proteins, homogenization still had a positive effect on fracture properties. Until the production process of commercial plant proteins is not tuned towards higher functionality, we should consider strategies to functionalize commercial plant protein isolates. In our upcoming work, we blend different plant proteins aiming for a synergistic effect in gel structures and we evaluate various enzymes (non-hydrolytic) to improve plant protein gelation properties. In these studies, we can use homogenization as a pre-treatment, as we have shown that homogenization is a valuable tool to improve gelation properties of commercial plant protein isolates in food applications.

## Funding sources

This work is part of the project 'Clean label solutions for structuring plant-based foods' co-financed by the Top Consortium for Knowledge and Innovation Agri & Food by the Dutch Ministry of Economic Affairs under contract number LWV20.68.

## CRedit authorship contribution statement

**Senna W.P.M. Janssen:** Writing – original draft, Validation, Methodology, Investigation, Conceptualization. **Laurice Pouvreau:** Writing – review & editing, Supervision, Methodology, Funding acquisition, Conceptualization. **Renko J. de Vries:** Writing – review & editing, Supervision, Methodology, Conceptualization.

## Declaration of competing interest

The authors declare that they have no known competing financial interests or personal relationships that could have appeared to influence the work reported in this paper.

## Data availability

Data will be made available on request.

## Appendix A. Supplementary data

Supplementary data to this article can be found online at <https://doi.org/10.1016/j.foodhyd.2024.110049>.

## References

- Aiking, H., & de Boer, J. (2020). The next protein transition. In *Trends in food science and technology* (Vol. 105, pp. 515–522). Elsevier Ltd. <https://doi.org/10.1016/j.tifs.2018.07.008>.
- Amaral, A. L., Ferreira, E. S., Silva, M. A., Neves, V. A., & Demonte, A. (2017). The Vicilin protein (*Vigna radiata* L.) of mung bean as a functional food: Evidence of “in vitro” hypocholesterolemic activity. *Nutrition & Food Science*, 47(6), 907–916. <https://doi.org/10.1108/NFS-05-2017-0089>
- Bader, S., Bez, J., & Eisner, P. (2011). Can protein functionalities be enhanced by high-pressure homogenization? – a study on functional properties of lupin proteins. *Procedia Food Science*, 1, 1359–1366. <https://doi.org/10.1016/j.profoo.2011.09.201>
- Baskinci, T., & Gul, O. (2023). Modifications to structural, techno-functional and rheological properties of sesame protein isolate by high pressure homogenization. *International Journal of Biological Macromolecules*, 250. <https://doi.org/10.1016/j.ijbiomac.2023.126005>
- Ben-Harb, S., Panouillé, M., Huc-Mathis, D., Moulin, G., Saint-Eve, A., Irlinger, F., et al. (2018). The rheological and microstructural properties of pea, milk, mixed pea/milk gels and gelled emulsions designed by thermal, acid, and enzyme treatments. *Food Hydrocolloids*, 77, 75–84. <https://doi.org/10.1016/j.foodhyd.2017.09.022>
- Berghout, J. A. M., Boom, R. M., & van der Goot, A. J. (2015). Understanding the differences in gelling properties between lupin protein isolate and soy protein isolate. *Food Hydrocolloids*, 43, 465–472. <https://doi.org/10.1016/j.foodhyd.2014.07.003>
- Bora, P. S., Brekke, C. J., & Powers, J. R. (1994). Heat induced gelation of pea (*Pisum sativum*) mixed globulins, vicilin and legumin. *Journal of Food Science*, 59(3), 594–596. <https://doi.org/10.1111/j.1365-2621.1994.tb05570.x>
- Burger, T. G., Singh, I., Mayfield, C., Baumert, J. L., & Zhang, Y. (2022). Comparison of physicochemical and emulsifying properties of commercial pea protein powders. *Journal of the Science of Food and Agriculture*, 102(6), 2506–2514. <https://doi.org/10.1002/jsfa.11592>
- Day, L., Cakebread, J. A., & Loveday, S. M. (2022). Food proteins from animals and plants: Differences in the nutritional and functional properties. In *Trends in food science and technology* (Vol. 119, pp. 428–442). Elsevier Ltd. <https://doi.org/10.1016/j.tifs.2021.12.020>.
- Ersch, C., Meinders, M. B. J., Bouwman, W. G., Nieuwland, M., van der Linden, E., Venema, P., et al. (2016). Microstructure and rheology of globular protein gels in the presence of gelatin. *Food Hydrocolloids*, 55, 34–46. <https://doi.org/10.1016/j.foodhyd.2015.09.030>
- Foegeding, E. A., Bowland, E. L., & Hardin, C. C. (1995). Factors that determine the fracture properties and microstructure of globular protein gels. *Topics in Catalysis*, 9(4), 237–249. [https://doi.org/10.1016/S0268-005X\(99\)80254-3](https://doi.org/10.1016/S0268-005X(99)80254-3)
- Ge, J., Sun, C., Chang, Y., Li, S., Zhang, Y., & Fang, Y. (2023). Understanding the differences in heat-induced gel properties of twelve legume proteins: A comparative study. *Food Research International*, 163. <https://doi.org/10.1016/j.foodres.2022.112134>
- Herz, E. M., Schäfer, S., Terjung, N., Gibis, M., & Weiss, J. (2021). Influence of transglutaminase on glucono- $\delta$ -lactone-induced soy protein gels. *ACS Food Science and Technology*, 1(8), 1412–1417. <https://doi.org/10.1021/acscfoodscitech.1c00102>
- Huang, Z. G., Wang, X. Y., Zhang, J. Y., Liu, Y., Zhou, T., Chi, S. Y., & Bi, C. H. (2022). High-pressure homogenization modified chickpea protein: Rheological properties, thermal properties and microstructure. *Journal of Food Engineering*, 335, Article 111196.
- Jo, Y. J., Huang, W., & Chen, L. (2020). Fabrication and characterization of lentil protein gels from fibrillar aggregates and the gelling mechanism study. *Food & Function*, 11(11), 10114–10125. <https://doi.org/10.1039/d0fo02089c>
- Johansson, M., Karkehabadi, S., Johansson, D. P., & Langton, M. (2023). Gelation behaviour and gel properties of the 7S and 11S globulin protein fractions from faba bean (*Vicia faba* var. minor) at different NaCl concentrations. *Food Hydrocolloids*, 142. <https://doi.org/10.1016/j.foodhyd.2023.108789>
- Johansson, M., Xanthakis, E., Langton, M., Menzel, C., Vilaplana, F., Johansson, D. P., et al. (2021). Mixed legume systems of pea protein and unrefined lentil fraction: Textural properties and microstructure. *LWT*, 144. <https://doi.org/10.1016/j.lwt.2021.111212>
- Kang, Z. L., Bai, R., Lu, F., Zhang, T., Gao, Z. S., Zhao, S. M., et al. (2022). Effects of high pressure homogenization on the solubility, foaming, and gel properties of soy 11S globulin. *Food Hydrocolloids*, 124. <https://doi.org/10.1016/j.foodhyd.2021.107261>
- Keuleyan, E., Gélébart, P., Beaumont, V., Kermarrec, A., Ribourg-Birault, L., Le Gall, S., et al. (2023). Pea and lupin protein ingredients: New insights into endogenous lipids and the key effect of high-pressure homogenization on their aqueous suspensions. *Food Hydrocolloids*, 141. <https://doi.org/10.1016/j.foodhyd.2023.108671>
- Kornet, R., Shek, C., Venema, P., Jan van der Goot, A., Meinders, M., & van der Linden, E. (2021). Substitution of whey protein by pea protein is facilitated by specific fractionation routes. *Food Hydrocolloids*, 117, Article 106691. <https://doi.org/10.1016/j.foodhyd.2021.106691>
- Langton, M., Ehsanzamir, S., Karkehabadi, S., Feng, X., Johansson, M., & Johansson, D. P. (2020). Gelation of faba bean proteins - effect of extraction method, pH and NaCl. *Food Hydrocolloids*, 103. <https://doi.org/10.1016/j.foodhyd.2019.105622>
- Levy, R., Okun, Z., Davidovich-Pinhas, M., & Shpigelman, A. (2021). Utilization of high-pressure homogenization of potato protein isolate for the production of dairy-free yogurt-like fermented product. *Food Hydrocolloids*, 113. <https://doi.org/10.1016/j.foodhyd.2020.106442>
- Luo, L., Cheng, L., Zhang, R., & Yang, Z. (2022). Impact of high-pressure homogenization on physico-chemical, structural, and rheological properties of quinoa protein isolates. *Food Structure*, 32. <https://doi.org/10.1016/j.foosr.2022.100265>



- Luo, L., Wang, Z., Deng, Y., Wei, Z., Zhang, Y., Tang, X., et al. (2022). High-pressure homogenization: A potential technique for transforming insoluble pea protein isolates into soluble aggregates. *Food Chemistry*, 397. <https://doi.org/10.1016/j.foodchem.2022.133684>
- Ma, Y., Zhang, J., He, J., Xu, Y., & Guo, X. (2023). Effects of high-pressure homogenization on the physicochemical, foaming, and emulsifying properties of chickpea protein. *Food Research International*, 170. <https://doi.org/10.1016/j.foodres.2023.112986>
- Martin, A. H., Nieuwland, M., & De Jong, G. A. H. (2014). Characterization of heat-set gels from RuBisCO in comparison to those from other proteins. *Journal of Agricultural and Food Chemistry*, 62(44), 10783–10791. <https://doi.org/10.1021/jf502905g>
- McCann, T. H., Guyon, L., Fischer, P., & Day, L. (2018). Rheological properties and microstructure of soy-whey protein. *Food Hydrocolloids*, 82, 434–441. <https://doi.org/10.1016/j.foodhyd.2018.04.023>
- Melchior, S., Moreton, M., Calligaris, S., Manzocco, L., & Nicoli, M. C. (2022). High pressure homogenization shapes the techno-functionalities and digestibility of pea proteins. *Food and Bioprocess Processing*, 131, 77–85. <https://doi.org/10.1016/j.fbp.2021.10.011>
- Mezger, T. G. (2014). *The rheology handbook. For users of rotational and oscillatory rheometers*. European Coatings Library.
- Moll, P., Salminen, H., Schmitt, C., & Weiss, J. (2021). Impact of microfluidization on colloidal properties of insoluble pea protein fractions. *European Food Research and Technology*, 247(3), 545–554. <https://doi.org/10.1007/s00217-020-03629-2>
- Moll, P., Salminen, H., Seitz, O., Schmitt, C., & Weiss, J. (2022). Characterization of soluble and insoluble fractions obtained from a commercial pea protein isolate. *Journal of Dispersion Science and Technology*. <https://doi.org/10.1080/01932691.2022.2093214>
- Nicolai, T., & Chassenieus, C. (2019). Heat-induced gelation of plant globulins. In \ (Vol. 27, pp. 18–22). Elsevier Ltd. <https://doi.org/10.1016/j.cofs.2019.04.005>
- Nivala, O., Mäkinen, O. E., Kruss, K., Nordlund, E., & Ercili-Cura, D. (2017). Structuring colloidal oat and faba bean protein particles via enzymatic modification. *Food Chemistry*, 231, 87–95. <https://doi.org/10.1016/j.foodchem.2017.03.114>
- Ong, K. S., Chiang, J. H., Sim, S. Y. J., Liebl, D., Madathummal, M., & Henry, C. J. (2022). Functionalising insoluble pea protein aggregates using high-pressure homogenisation: Effects on physicochemical, microstructural and functional properties. *Food Structure*, 34. <https://doi.org/10.1016/j.foostr.2022.100298>
- Renkema, J. M. S., Knabben, J. H. M., & Van Vliet, T. (2001). Gel formation by b-conglycinin and glycinin and their mixtures. *Food Hydrocolloids*, 15(4–6), 407–414. [www.elsevier.com/locate/foodhyd](http://www.elsevier.com/locate/foodhyd)
- Sahil, Madhumita, M., Prabhakar, P. K., & Kumar, N. (2022). Dynamic high pressure treatments: Current advances on mechanistic-cum-transport phenomena approaches and plant protein functionalization. *Critical Reviews in Food Science and Nutrition*, 1–26.
- Saricaoglu, F. T. (2020). Application of high-pressure homogenization (HPH) to modify functional, structural and rheological properties of lentil (*Lens culinaris*) proteins. *International Journal of Biological Macromolecules*, 144, 760–769. <https://doi.org/10.1016/j.ijbiomac.2019.11.034>
- Saricaoglu, F. T., Gul, O., Besir, A., & Atalar, I. (2018). Effect of high pressure homogenization (HPH) on functional and rheological properties of hazelnut meal proteins obtained from hazelnut oil industry by-products. *Journal of Food Engineering*, 233, 98–108. <https://doi.org/10.1016/j.jfoodeng.2018.04.003>
- Shand, P. J., Ya, H., Pietrasik, Z., & Wanasundara, P. K. J. P. D. (2007). Physicochemical and textural properties of heat-induced pea protein isolate gels. *Food Chemistry*, 102(4), 1119–1130. <https://doi.org/10.1016/j.foodchem.2006.06.060>
- Sharan, S., Zanghelini, G., Zotzel, J., Bonerz, D., Aschoff, J., Saint-Eve, A., et al. (2021). Fava bean (*Vicia faba* L.) for food applications: From seed to ingredient processing and its effect on functional properties, antinutritional factors, flavor, and color. *Comprehensive Reviews in Food Science and Food Safety*, 20(1), 401–428. <https://doi.org/10.1111/1541-4337.12687>
- Shkolnikov Lozober, H., Okun, Z., & Shpigelman, A. (2021). The impact of high-pressure homogenization on thermal gelation of *Arthrospira platensis* (Spirulina) protein concentrate. *Innovative Food Science and Emerging Technologies*, 74. <https://doi.org/10.1016/j.ifset.2021.102857>
- Stading, M., & Hermansson, A. M. (1991). Large deformation properties of  $\beta$ -lactoglobulin gel structures. *Food Hydrocolloids*, 5(4), 339–352. [https://doi.org/10.1016/S0268-005X\(09\)80046-5](https://doi.org/10.1016/S0268-005X(09)80046-5)
- Sun, D., Wu, M., Bi, C., Gao, F., Wei, W., & Wang, Y. (2022). Using high-pressure homogenization as a potential method to pretreat soybean protein isolate: Effect on conformation changes and rheological properties of its acid-induced gel. *Innovative Food Science & Emerging Technologies*, 82, Article 103195. <https://doi.org/10.1016/j.ifset.2022.103195>
- Sun-Waterhouse, D., Zhao, M., & Waterhouse, G. I. N. (2014). Protein modification during ingredient preparation and food processing: Approaches to improve food processability and nutrition. *Food and Bioprocess Technology*, 7(7), 1853–1893. <https://doi.org/10.1007/s11947-014-1326-6>. Springer New York LLC.
- Tang, C. H., & Sun, X. (2010). Physicochemical and structural properties of 8S and/or 11S globulins from mungbean [*Vigna radiata* (L.) Wilczek] with various polypeptide constituents. *Journal of Agricultural and Food Chemistry*, 58(10), 6395–6402. <https://doi.org/10.1021/jf904254f>
- Tang, C. H., Wang, X. Y., Yang, X. Q., & Li, L. (2009). Formation of soluble aggregates from insoluble commercial soy protein isolate by means of ultrasonic treatment and their gelling properties. *Journal of Food Engineering*, 92(4), 432–437. <https://doi.org/10.1016/j.jfoodeng.2008.12.017>
- Tanger, C., Müller, M., Andlinger, D., & Kulozik, U. (2022). Influence of pH and ionic strength on the thermal gelation behaviour of pea protein. *Food Hydrocolloids*, 123, Article 106903. <https://doi.org/10.1016/J.FOODHYD.2021.106903>
- van Vliet, T. (1996). Large deformation and fracture behaviour of gels. *Current Opinion in Colloid & Interface Science*, 1(6), 740–745. [https://doi.org/10.1016/S1359-0294\(96\)80075-6](https://doi.org/10.1016/S1359-0294(96)80075-6)
- Van Vliet, T., & Walstra, P. (1995). Large deformation and fracture behaviour of gels. *Faraday Discussions*, 101.
- Vogelsang-O'Dwyer, M., Petersen, I. L., Joehnke, M. S., Sørensen, J. C., Bez, J., Detzel, A., et al. (2020). Comparison of Faba bean protein ingredients produced using dry fractionation and isoelectric precipitation: Techno-functional, nutritional and environmental performance. *Foods*, 9(3). <https://doi.org/10.3390/foods9030322>
- Warsame, A. O., Michael, N., O'Sullivan, D. M., & Tosi, P. (2020). Identification and quantification of major faba bean seed proteins. *Journal of Agricultural and Food Chemistry*, 68(32), 8535–8544. <https://doi.org/10.1021/acs.jafc.0c02927>
- Yang, Q., Eikelboom, E., van der Linden, E., de Vries, R., & Venema, P. (2022). A mild hybrid liquid separation to obtain functional mungbean protein. *LWT*, 154. <https://doi.org/10.1016/j.lwt.2021.112784>
- Yang, J., Liu, G., Zeng, H., & Chen, L. (2018). Effects of high pressure homogenization on faba bean protein aggregation in relation to solubility and interfacial properties. *Food Hydrocolloids*, 83, 275–286. <https://doi.org/10.1016/j.foodhyd.2018.05.020>
- Yang, J., Mocking-Bode, H. C. M., van den Hoek, I. A. F., Theunissen, M., Voudouris, P., Meinders, M. B. J., et al. (2022). The impact of heating and freeze or spray drying on the interface and foam stabilising properties of pea protein extracts: Explained by aggregation and protein composition. *Food Hydrocolloids*, 133. <https://doi.org/10.1016/j.foodhyd.2022.107913>
- Zhao, X., Liu, X., & Xue, F. (2023). Effects of high-pressure homogenization treatment on physicochemical properties of novel plant proteins. *Applied Food Research*, 3(1), Article 100285. <https://doi.org/10.1016/j.afres.2023.100285>